Journal of Materials Chemistry C

PAPER

Check for updates

Cite this: J. Mater. Chem. C, 2017, 5, 11758

Enhancement of hole mobility in hybrid titanium dioxide/poly(3-hexylthiophene) nanocomposites by employing an oligothiophene dye as an interface modifier†

K. Prashanthan,[a] T. Thivakarasarma,[a] P. Ravirajan,*[a] M. Planells,[b] N. Robertson[b] and J. Nelson[c]

Received 20th May 2017,
Accepted 28th September 2017

DOI: 10.1039/c7tc02225e

rsc.li/materials-c

This study focuses on the influence of interface modifiers on the charge transport of hybrid nanoporous titanium dioxide (TiO_2)/poly(3-hexylthiophene) (P3HT) nanocomposites by using the time of flight technique. We found that the hole-mobility in the nanocomposites is about three orders of magnitude less than that of pristine P3HT. This may be due to poor infiltration of the polymer into the highly structured porous TiO_2 which in turn obstructs the charge transport of the carriers. However, the hole-mobility in the nanocomposites is increased by an order of magnitude when a ruthenium based dye, either Z907 or N719, is introduced at the TiO_2/P3HT interface. Surprisingly, the electron-mobility of the composite is decreased upon dye treatment. We further observed that the hole-mobility of nanocrystalline TiO_2/P3HT composites treated with a 3-hexylthiophene derivative with a cyanoacrylic acid group [(*E*)-2-cyano-3-(3′,3″,3‴-trihexyl-[2,2′:5′,2″:5″,2‴-quaterthiophene]-5-yl)acrylicacid] (4T) increased to over 10^{-5} cm^2 V^{-1} s^{-1}, which is over an order of magnitude higher than the hole-mobility found in untreated nanocomposites. This trend in hole-mobility is consistent with corresponding current density (*J*)–voltage (*V*) characteristics under illumination of TiO_2/P3HT devices with or without a dye interface layer. The higher hole-mobility found in the 4T dye treated TiO_2/P3HT nanocomposite is assigned to passivation of surface traps by the dye as well as improved packing of the polymer with the nanocrystals through effective inter-chain interactions of 4T with P3HT.

Introduction

Organic photovoltaic devices based on metal oxide/polymer nanocomposites have attracted extensive interest due to their high mechanical stability and the multiple routes available to control the interface morphology.[1–5] However performance improvements are needed to improve the power conversion efficiency of photovoltaic devices, which have until now been limited by poor infiltration of conjugated polymers into porous metal oxide films[6] and by poor charge transport in metal oxide/polymer nanocomposites.[7,8] Studies of the transport properties are of fundamental importance in interpreting the basic physics in molecular PV devices,[9] in particular, the collection efficiency of photogenerated charges, and thus in enhancing the performance of such devices. It is generally difficult to determine the charge carrier mobility uniquely[10–12] in organic or hybrid semiconductors because of the high degree of energetic (diagonal) and structural (off-diagonal) disorder. Time of flight (TOF) transient photocurrent is an established technique[13–15] for mobility measurement in high-resistivity materials that allows these types of disorder to be quantified. Although a few independent studies have reported the electron mobility in porous TiO_2[7] and hole-mobility in poly(3-hexylthiophene) (P3HT),[12,16] no TOF studies of TiO_2/P3HT nanocomposites have been reported so far. Transport in organic/inorganic nancomposites is interesting because the combination of materials may affect charge transport in different ways, for example, through the restriction of charge percolation pathways, the effect of the composite on molecular packing in the organic component, and the effect of interactions between charge carriers and the interface.

Several strategies have been used to modify the metal oxide surface in order to improve the electronic properties of metal oxide/polymer hybrid materials, including the use of CdS quantum dots (QDs)[17] and the control of polymer alignment

[a] Department of Physics, University of Jaffna, Jaffna, Sri Lanka. E-mail: pravirajan@univ.jfn.ac.lk, pravirajan@gmail.com
[b] EaStCHEM School of Chemistry, University of Edinburgh, Joseph Black Building, Edinburgh EH9 3FJ, UK
[c] Department of Physics, Imperial College London, Prince Consort Road, London SW7 2BZ, UK

† Electronic supplementary information (ESI) available. See DOI: 10.1039/c7tc02225e

within the pores of the oxide structure.[18] It has also been reported that a thin overlayer of alumina[19] retards recombination kinetics in hybrid TiO_2–P3HT solar cells as well as in dye sensitized solar cells[20–22] and thus improves the overall cell performance. More recently, it has been shown that the overall device performance of TiO_2/polymer solar cells can be enhanced by more than a factor of two using a self-assembled monolayer[23] on TiO_2 nanoparticles with a permanent dipole pointing towards the TiO_2 surface or pointing towards the polymer when compared to a control device with no interface modifiers. It has also been demonstrated that inter dye hole-transport[24–26] may contribute to current collection in solid-state dye-sensitized solar cells.

In the present work, we focus on studying the effect on hole transport in hybrid titanium dioxide/polythiophene (P3HT) nanocomposites of sensitizing the surface of the titanium dioxide with a monolayer of conjugated dye molecules, using ruthenium (Ru) based dyes (Z907 and N719) and a carboxylated thiophene oligomer, (*E*)-2-cyano-3-(3′,3″,3‴-trihexyl-[2,2′:5′,2″:5″,2‴-quaterthiophene]-5-yl) acrylicacid (4T)[27] as interface modifiers. The chemical structures and full names of the dyes used in this study are shown in Fig. 1. We use TOF as a tool to determine the carrier mobilities of the nanocomposites with or without interface modifiers. We find that the addition of the modifier increases the TOF hole mobility by up to two orders of magnitude. The effect of interface properties on the electronic properties of an adjacent semiconductor is more broadly relevant, for example, to the phenomena of charge recombination or charge trapping at interfaces in electronic devices. The finding is therefore relevant to the understanding and control of interfaces in organic and hybrid electronic devices.

Experimental

Sample preparation

The samples were prepared on patterned Indium Tin Oxide (ITO) coated glass substrates (12 mm × 12 mm, 10 Ω square^{-1}), which were cleaned similarly to those reported elsewhere.[28] The substrates were then covered with a dense TiO_2 hole-blocking layer of 50 nm thickness by spray pyrolysis. For deposition of the porous TiO_2 layer, TiO_2 paste (DSL 18NRT, Dyesol) having colloids of ∼20 nm diameter was dissolved in tetrahydrofuran (THF) (180 mg ml^{-1}) and deposited on ITO substrates already coated with a dense TiO_2 layer by spin coating a TiO_2/THF solution (180 mg ml^{-1}) followed by sintering at 450 °C. The dye was then introduced at the polymer/TiO_2 interface by first heating the porous TiO_2 films at 110 °C for 10 minutes to remove surface water, followed by dipping the porous TiO_2 films in a 0.3 mM solution of the respective dye (Z907; M_w = 870.10, N719; M_w = 1188.75 both purchased from Dyesol, or 4T, synthesized as described in ref. 27) in a solvent consisting of acetonitrile : *tert*-butanol (1 : 1 by volume), for 14 hours. The samples were then rinsed in acetonitrile : *tert*-butanol solution and dried in nitrogen followed by dipping in P3HT polymer (M_n = 24 000; M_w: 55 000; RR = 95% purchased from Merck Chemicals Ltd) solution dissolved in chlorobenzene (2 mg ml^{-1}), overnight at 120 °C prior to P3HT spin coating, in order to obtain an active layer thickness of about 1 μm. Subsequently, these samples were coated with an 40 nm layer of highly-conductive poly(3,4-ethylenedioxythiophene)-poly(styrenesulfonate)(PEDOT:PSS)[29] by spin coating before depositing a Au top contact of 40 nm by thermal evaporation through a shadow mask under high vacuum. Finally, silver paste was applied and annealed to improve the contacts during measurements.

Characterization of the samples

The optical absorption spectra of the Z907, N719 and 4T coated nanoporous TiO_2 electrodes and spectra of the Z907, N719 and 4T treated TiO_2 samples that had been coated with P3HT by dip and spin coating were measured using a JENWAY-6800 UV-Vis spectrometer. For charge transport studies of the nanocomposite devices, completed as described above, charge pairs were generated optically with a frequency-doubled Nd:YAG laser (excitation wavelength 532 nm, pulse width less than 6 ns, energy per pulse ∼10 μJ, repetition rate 1 Hz and nominal beam diameter 2–8 mm), illuminating through the ITO. The photocurrent

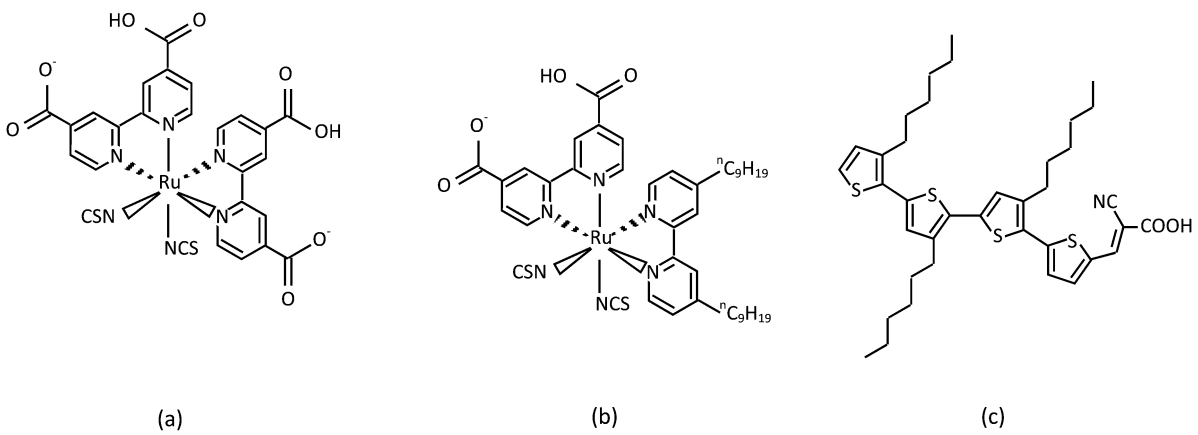

Fig. 1 Chemical structure of (a) di-tetrabutylammonium *cis*-bis(isothiocyanato)bis(2,2′-bipyridyl-4,4′-dicarboxylato)ruthenium(II) (N719), (b) tetrabutylammonium *cis*-bis(isothiocyanato)(2,2′-bipyridyl-4,4′-dicarboxylato)(4,4′-di-nonyl-2′-bipyridyl)ruthenium(II) (Z907) and (c) (*E*)-2-cyano-3-(3′,3″,3‴-trihexyl-[2,2′:5′,2″:5″,2‴-quaterthiophene]-5-yl)acrylicacid (4T).

transients were monitored with a TDS 1012B (Two channel Digital Storage oscilloscope) maintaining the ITO terminal at positive potential for finding the hole-mobility and at negative potential for the electron mobility.

Results and discussion

Fig. 2(a) shows the optical absorption spectra of porous TiO_2 (600 nm)/dye (ruthenium dyes or 4T), the porous TiO_2 (600 nm)/dye/P3HT ternary systems and the corresponding untreated porous TiO_2 (600 nm)/P3HT binary system and Fig. 2(b) shows the absorption spectra of the corresponding dye in acetonitrile : *tert*-butanol (1 : 1 by volume) (0.06 mM). Although the peak absorbance of the 4T dye solution is found at 470 nm,[27] the peak optical absorption of the 4T dye treated porous TiO_2 (600 nm) film is shifted towards 440 nm, which suggests a disruption of the packing of 4T oligomers due to an interaction between 4T and the TiO_2 surface.

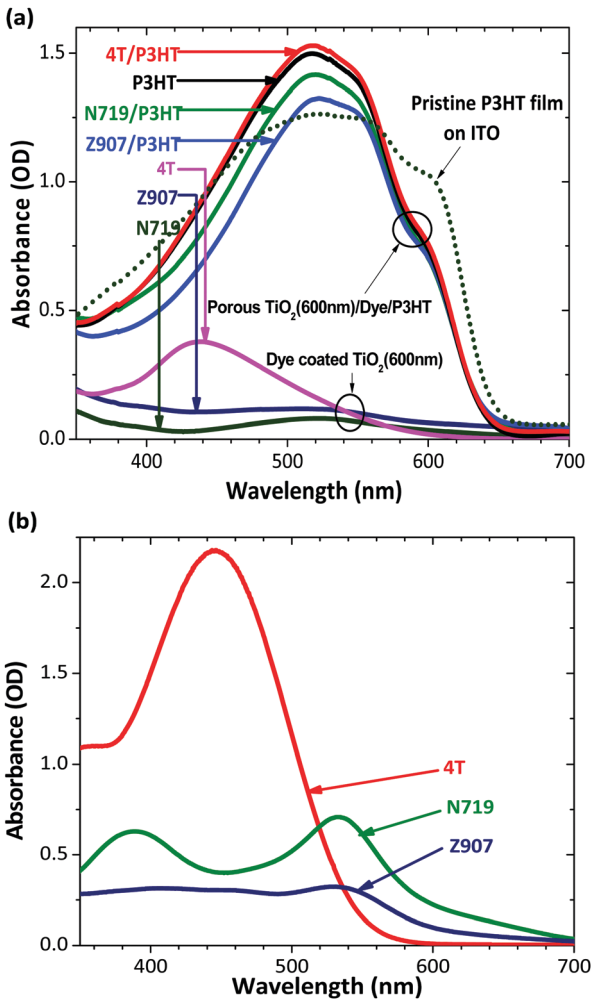

Fig. 2 (a) Optical absorption spectra of porous TiO_2 (600 nm)/dye (ruthenium dyes, 4T), porous TiO_2 (600 nm)/dye/P3HT ternary systems and the corresponding untreated porous TiO_2 (600 nm)/P3HT binary system and (b) absorption spectra of each of the three dyes in acetonitrile : *tert*-butanol (1 : 1 by volume) (0.06 mM).

A comparison of the optical absorption spectra of the porous TiO_2 (600 nm)/dye/P3HT ternary systems and the corresponding porous TiO_2 (600 nm)/dye binary system shows that all dye coated TiO_2 films have weak absorption (OD $\sim$ 0.15) in comparison with absorption of TiO_2/dye/P3HT films (OD $\sim$ 1.5) at the pumping wavelength of 532 nm though 4T treated porous TiO_2 films have significant absorption near to the blue wavelength. It could also be clearly seen that the absorption spectra of the untreated and treated films do not show any significant differences in their shape except for a small increase or decrease in absorption. This indicates that the microstructure of P3HT within a P3HT/TiO_2 composite is not strongly affected by the presence of these modifiers. However, comparison of absorption spectra for the pristine P3HT and dye coated composites in Fig. 2(a) shows that the packing of P3HT is apparently affected by the combination of the polymer with the TiO_2.

The sharper absorption edge in the red region shown in the spectrum of pristine P3HT on ITO compared to those of the P3HT coated films (Fig. 2(a)) suggests that the molecular packing of the polymer in the hybrid TiO_2 structures is disrupted somewhat relative to the pristine state.

In order to study the charge carrier mobilities in the composite samples, we used the time of flight (TOF) photocurrent technique to study the samples of the structure ITO/dense TiO_2/active layer/PEDOT:PSS/Au where the active layer is porous TiO_2 or a TiO_2/P3HT nanocomposite. In TOF, short laser pulses illuminate the sample through the TiO_2 electrode and so create a layer of electron–hole pairs in the polymer near the TiO_2 layers. The ITO is maintained either at positive potential for finding the hole-mobility or at negative potential for the electron mobility, such that charge carriers of sign opposite to that being studied are rapidly pulled towards the ITO/TiO_2 electrode, leaving the charge carriers of interest to drift across the samples towards the Au electrode under the influence of the electric field. The drifting photo-generated carriers then constitute an induced photocurrent transient which is analyzed to determine the charge transit time at that applied field and hence to find the electron or hole mobility in the composite film.

We study the following structures, (A) ITO/dense TiO_2/porous TiO_2 (600 nm)/PEDOT:PSS/Au, (B) ITO/dense TiO_2/porous TiO_2 (600 nm)/P3HT (250 nm)/PEDOT:PSS/Au, and (C) ITO/dense TiO_2/porous TiO_2 (600 nm)/dye/P3HT (250 nm)/PEDOT:PSS/Au, using each of the three dyes. Here the dense TiO_2 and PEDOT:PSS layers serve as hole- and electron- blocking layers, respectively. Since the steady state absorption due to the dye in the nanocomposite at the pumping wavelength of 532 nm is significantly lower than the absorption of the porous TiO_2/dye/P3HT nanocomposites (see Fig. 2(b)), we can safely neglect the carrier generation in the dye and its contribution to the charge transport in the active layer. Fig. 2(a) confirms that all the samples are optically thick at the pumping wavelength of 532 nm, which is a necessary condition to determine carrier mobilities precisely by TOF.

The attempt to draw the holes in porous TiO_2 (structure A) by applying positive voltage to the illuminated transparent electrode was not successful even at very high voltage. This observation

indicates that the hole-mobility of porous TiO_2 is very low. A photocurrent transient was observed when a negative voltage was applied to the illuminated ITO. This photocurrent transient was assigned to electron transport.

Fig. 3(a) shows hole photocurrent transients at an applied field of 1.6×10^{-5} V m^{-1} for untreated (TiO_2/P3HT) (structure B) and treated structures (TiO_2/4T dye/P3HT) (structure C). Because of the absence of a hole photocurrent in structure A, we may safely assign the photocurrents in structures B and C to hole transport in the polymer phase. All transients are dispersive, possessing a monotonic decay with a change in gradient around a characteristic "knee" on a double logarithmic plot [Fig. 3(a)]. Dispersive transport is typically assigned to trapping and de-trapping of charges from an energetic distribution of trap states during transit,[30–32] and this is likely to be the reason for the dispersive transport in the case of these nanocomposites.

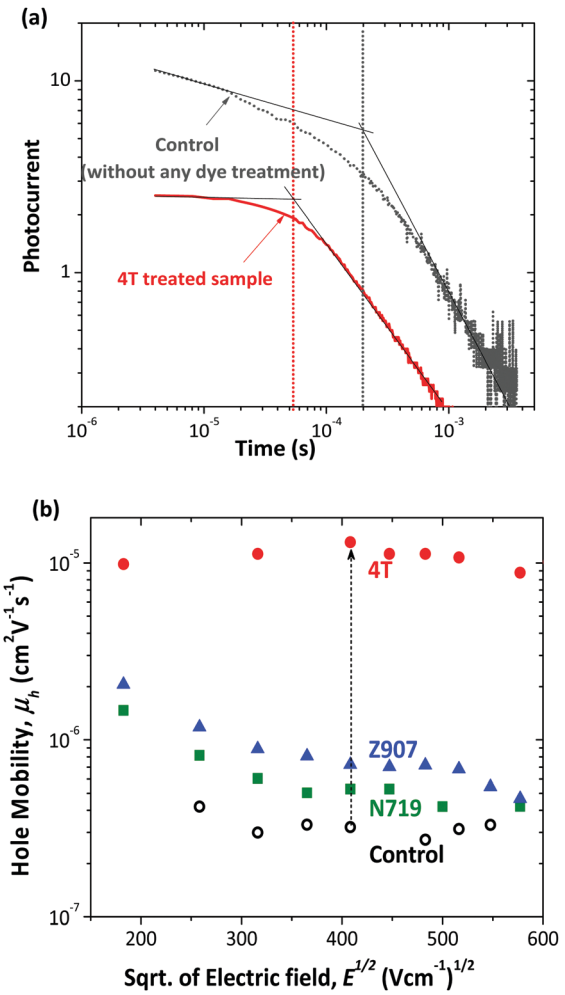

Fig. 3 (a) The hole photocurrent transients at an applied field of 1.6×10^{-5} V m^{-1} for untreated (TiO_2/P3HT) (dashed line) and treated structures (TiO_2/4T dye/P3HT) (solid line) and (b) the electric-field dependence of drift mobility in TiO_2/P3HT samples with and without interface modification. Filled circle for 4T, triangle for Z907, square for N719 treated films and open circle for TiO_2/P3HT with no modifier (control).

Fig. 3(a) shows that the hole-transient is around an order of magnitude faster in the 4T treated structure than the untreated one. Fig. 3(b) shows the hole mobility as a function of applied electric field for unmodified films and films modified with each of the three dyes. The hole mobility in the structure without a dye interface layer is on the order of 10^{-7} cm^2 V^{-1} s^{-1}. This is comparable with the reported values for some polymer/fullerene derivative devices obtained using TOF[10,33] but is more than two orders of magnitude less than that of pristine P3HT where the hole-mobility has been reported as 3.0×10^{-4} cm^2 V^{-1} s^{-1}.[16] The poor hole transport may be due to disrupted packing of P3HT in the porous structure or to discontinuous pathways due to the TiO_2 mesostructure. However this poor hole mobility was increased by a factor of 2–5 when Ru based dyes were applied, and by over an order of magnitude when 4T was applied to the same porous TiO_2 matrix. Therefore the hole transport is influenced by the nature of the interface modifier and not only by the TiO_2 mesostructure. Fig. 3(b) also shows that only 4T treated films show more or less electric field independent mobility. Fig. S3(d) in the ESI† compares time-of-flight profiles for 4T samples of two different thicknesses at the same applied electric field. The similar hole-mobility values in thin and thick samples support the assumption of a uniform electric field and validate the TOF mobility values.

We now address the reasons for the higher hole-mobility in the dye treated, and particularly the 4T treated, composite films. One possible explanation is that the dye changes the surface energy of the TiO_2 surface to improve compatibility with P3HT and assist insertion of the polymer phase, which would lead to more continuous pathways for hole-transport[1] and so increase mobility. This idea is supported by measurements of the contact angle of water with the untreated and dye-treated TiO_2 surface shown in the ESI,† Fig. S5, which shows that the surface becomes much more hydrophobic upon dye treatment, and therefore more compatible with P3HT. There is no evidence from the optical absorption in Fig. 2(a) to support a strong difference in the polymer microstructure when using different dyes or no dyes, however, the composite absorption spectrum need not be correlated to pore penetration. Another effect of the dye layer could be to remove electrons by facilitating electron injection into TiO_2 after exciton generation and so reduce the probability of hole recombination during transit. The LUMO energies of N719 and Z907 relative to P3HT[1,34] would allow the dyes to serve as a shuttle for electron transfer to TiO_2, and electron injection from these dyes into TiO_2 is known to be efficient.

Regarding the striking enhancement in the hole-mobility of over an order of magnitude in 4T treated nanocomposite films compared to untreated films, we propose that this effect may be explained by the compatibility between the chemically similar P3HT and 4T chains, which is likely to lead to an attractive interaction between polymers and molecules. Such interaction between dissimilar thiophene chains is analogous to the inter chain aggregation which is known to occur in P3HT polymer films and the aggregation within 4T in solution that was suggested by the spectra in Fig. 2(a) and (b) above. This reasoning supports the idea that the 4T dye improves the penetration of polymer

into the pores of TiO_2 leading to a more continuous polymer phase for hole-transport than in the absence of the dye. The higher hole-mobility is consistent with the higher photocurrent generation efficiency that is observed in TiO_2/P3HT photovoltaic devices when the TiO_2 surface is coated with the respective dyes (ESI,† Fig. S4(a) and (b)).

Conclusions

Hole-mobility improvements in hybrid TiO_2/P3HT nanocomposites employing interface modifiers have been studied using the time-of-flight photocurrent technique. The hole mobility in the nanocomposite was improved by a factor of 2–5 relative to the unmodified TiO_2/P3HT system when Ru based dyes (N719 and Z907) were introduced at the interface, and by over an order of magnitude when a quaterthiophene based dye (4T) was used. The strong effect of the 4T dye, which is chemically similar to the polymer, suggests that a dye–polymer interaction may assist in pore filling by the polymer and establish more continuous pathways for hole-transport. The hole mobility in the composite in the presence of the 4T dye is over 10^{-5} cm^2 V^{-1} s^{-1} which is only an order of magnitude smaller than that in pristine P3HT polymer. Dyes may also assist hole-transport by facilitating electron injection into TiO_2 and reducing hole loss by recombination. Further studies are needed to clarify the mechanism of improved hole-transport. We conclude that interface modification using carefully chosen dyes may significantly improve hole-mobility in hybrid TiO_2/P3HT nanocomposites.

Author contributions

K. P. and P. R. designed and organized the project, developed interpretation of the results and wrote the manuscript. K. P. and T. T. fabricated the solar cell devices, and carried out optical and electrical characterization, TOF experiments and data analysis. M. P. and N. R. carried out the synthesis and design of the 4T polymer. P. R., N. R. and J. N. developed the interpretation of the results and supported the writing of the manuscript.

Conflicts of interest

There are no conflicts to declare.

Acknowledgements

KP and PR acknowledge the University of Jaffna, Sri Lanka and Norwegian Centre for International Cooperation in Education (SIU) for research project grants numbers URG/2016/SEIT/09 and NORPART-2016/10237. NR and JN thank EPSRC for project grant numbers EP/M023532/1 (NR) and EP/K010298/1 and EP/P02484X/1 (JN).

Notes and references

1 P. Ravirajan, *et al.*, *J. Phys. Chem. B*, 2006, **110**, 7635–7639.
2 M. He, F. Qiu and Z. Lin, *J. Phys. Lett.*, 2013, **4**, 1788–1796.
3 Z. Wang, *et al.*, *Appl. Surf. Sci.*, 2008, **255**, 1916–1920.
4 J. Weickert, *et al.*, *J. Phys. Chem. C*, 2011, **115**, 15081–15088.
5 P. Atienzar, *et al.*, *J. Phys. Lett.*, 2010, **1**, 708–713.
6 P. Ravirajan, *et al.*, *Thin Solid Films*, 2004, **451**, 624–629.
7 B. O. Aduda, *et al.*, *Int. J. Photoenergy*, 2004, **6**, 141–147.
8 J. Nelson, *Phys. Rev. B: Condens. Matter Mater. Phys.*, 1999, **59**, 15374.
9 J. Nelson, J. Kirkpatrick and P. Ravirajan, *Phys. Rev. B: Condens. Matter Mater. Phys.*, 2004, **69**, 035337.
10 S. Choulis, *et al.*, *Appl. Phys. Lett.*, 2003, **83**, 3812–3814.
11 R. Mauer, M. Kastler and F. Laquai, *Adv. Funct. Mater.*, 2010, **20**, 2085–2092.
12 K. Yang, *et al.*, *J. Macromol. Sci., Part A: Pure Appl. Chem.*, 2007, **44**, 1261–1264.
13 D. Poplavskyy and J. Nelson, *J. Appl. Phys.*, 2003, **93**, 341–346.
14 P. Ravirajan, *et al.*, *Adv. Funct. Mater.*, 2005, **15**, 609–618.
15 T. Yoshikawa, *et al.*, *Thin Solid Films*, 2008, **516**, 2595–2599.
16 S. Choulis, *et al.*, *Appl. Phys. Lett.*, 2004, **85**, 3890–3892.
17 M. Thanihaichelvan, *et al.*, *J. Mater. Sci.: Mater. Electron.*, 2015, **26**, 3558–3563.
18 K. M. Coakley, *et al.*, *Adv. Funct. Mater.*, 2005, **15**, 1927–1932.
19 S. Loheeswaran, *et al.*, *J. Nanoelectron. Optoelectron.*, 2013, **8**, 484–488.
20 E. Palomares, *et al.*, *J. Am. Chem. Soc.*, 2003, **125**, 475–482.
21 Y. Hu, *et al.*, *J. Mater. Chem. A*, 2016, **4**, 2509–2516.
22 A. Abate, *et al.*, *Adv. Energy Mater.*, 2014, **4**, 1400166.
23 S. Loheeswaran, *et al.*, *J. Mater. Sci.: Mater. Electron.*, 2017, **28**, 4732.
24 D. Moia, *et al.*, *Adv. Mater.*, 2015, **27**, 5889–5894.
25 D. Moia, *et al.*, *J. Phys. Chem. C*, 2015, **119**, 18975–18985.
26 R. A. Krüger, *et al.*, *ACS Appl. Mater. Interfaces*, 2011, **3**, 2031–2041.
27 M. Planells, *et al.*, *ACS Appl. Mater. Interfaces*, 2014, **6**, 17226–17235.
28 P. Ravirajan, *et al.*, *J. Appl. Phys.*, 2004, **95**, 1473–1480.
29 S. Rutledge and A. Helmy, *J. Appl. Phys.*, 2013, **114**, 133708.
30 B. C. O'Regan and J. R. Durrant, *J. Phys. Chem. B*, 2006, **110**, 8544–8547.
31 A. Janotti, *et al.*, *Phys. Rev. B: Condens. Matter Mater. Phys.*, 2010, **81**, 085212.
32 J. Varley, *et al.*, *Phys. Rev. B: Condens. Matter Mater. Phys.*, 2012, **85**, 081109.
33 V. D. Mihailetchi, *et al.*, *Adv. Funct. Mater.*, 2006, **16**, 699–708.
34 I. Chung, *et al.*, *Nature*, 2012, **485**, 486–489.

